Received: 4 March 2022 | Revised: 24 May 2022 | Accepted: 21 June 2022

DOI: 10.1002/jemt.24198

RESEARCH ARTICLE

MICROSCOPY RESEARCH & TECHNIQUE WILEY

Focus variation due to near infrared laser in a confocal microscope

Melissa Matrecitos-Avila[1] | Remy Avila[1] | Reinher Pimentel-Domínguez[1] | Salvador Cuevas[2] | Elisa Tamariz[3] | Pablo Loza-Alvarez[4]

[1]Centro de Física Aplicada y, Tecnología Avanzada, Universidad Nacional Autónoma de México (UNAM), Querétaro, Mexico

[2]Instituto de Astronomía, Universidad Nacional Autónoma de México (UNAM), CDMX, Mexico

[3]Instituto de Ciencias de la Salud, Universidad Veracruzana, Veracruz, Mexico

[4]ICFO-Institut de Ciencies Fotoniques, The Barcelona Institute of Science and Technology, Barcelona, Spain

Correspondence
Remy Avila, Centro de Física Aplicada y Tecnología Avanzada, Universidad Nacional Autónoma de México (UNAM), Querétaro, Mexico.
Email: remy@fata.unam.mx

Funding information
Consejo Nacional de Ciencia y Tecnología, Grant/Award Number: FORDECYT-PRONACES/1561826; Dirección General de Asuntos del Personal Académico, Universidad Nacional Autónoma de México, Grant/Award Numbers: IN111815, IN108420, postdoctoral grant; Fundación Cellex; Fundación Mig-Puig; Generalitat de Catalunya; Laserlab-Europe, Grant/Award Number: 871124; Ministerio de Economía y Competitividad, Grant/Award Number: SEV-2015-0522; Secretaría de Educación Pública

Review Editor: Alberto Diaspro

Abstract

Focus precision and stability is crucial in confocal microscopy not only for image sharpness but also to avoid radiometric fluctuations that can wrongly be interpreted as variations of the fluorescence intensity in the sample. Here we report a focus variation provoked by a continuous wave laser of 810-nm wavelength introduced along the optical path of an inverted confocal microscope with an oil immersion ×60 objective. When the laser is turned on or off, the focus position drifts toward lower or high values of the vertical coordinate *z*, respectively. The maximum drift observed was 2.25 μm for a laser power of 40 mW at the sample and over a 600-s exposure time. The temporal evolution of the focus position is well fitted by exponential curves that mimic temperature variations due to a heat source. Our analysis strongly suggests that the focus drift is due to heating of the immersion oil.

KEYWORDS
confocal microscopy, near infrared laser, optical tweezers

Research Highlights

We report the change in focus position provoked by a continuous-wave 810-nm laser focalized on a sample through the objective of a confocal microscope. Our results and analysis are consistent with the immersion oil being heated by the laser, which modifies the oil refractive index with a consequent noticeable focus drift.

1 | INTRODUCTION

Confocal fluorescence microscopy is a powerful tool in different scientific fields like biology and biomedicine. The principal feature of this technique is that only light emerging from the focal plane of the microscope objective contributes to the image, while out-of-focus light is suppressed. By acquiring images at different planes, it is possible to reconstruct 3D images of the sample (Jerome & Price, 2018; Jonkman et al., 2020; Jonkman & Brown, 2015). There are several kinds of confocal microscopes, but the most commonly used is the confocal laser-scanning microscope, in which a laser is scanned over the sample to excite fluorescent molecules. The signal is then collected point by point to generate an image (Jonkman & Brown, 2015). Confocal microscopy has been used in diverse contexts

like the study of cells (Stephens & Allan, 2003), to image organs in live animals (Marques et al., 2015), in ophthalmology (Erie et al., 2009), for diagnosis in oncology (Guida et al., 2021), to cite but a few.

Confocal microscopy can be used in combination with other optical techniques with either the very same instrumentation or adapting other optical elements. For example, together with fluorescence confocal microscopy, a near infrared (NIR) laser can be used for trapping micron-scale objects in an optical tweezers configuration (Curran et al., 2014; Hoffmann et al., 2000; Visscher et al., 1993; Visscher & Brakenhoff, 1991; Vossen et al., 2004; Yevnin et al., 2013). The two techniques can be implemented in different microscope objectives, putting the sample between them (Visscher et al., 1993; Vossen et al., 2004; Yevnin et al., 2013) or the NIR laser for optical trapping can be inserted into the confocal microscope using a dichroic mirror and use the same objective for trapping, exciting and imaging (Visscher & Brakenhoff, 1991; Hoffmann et al., 2000; Curran et al., 2014; Nemet et al., 2002). This combination allows controlling micron-size objects in three dimensions and to capture a three-dimensional image at the same time. By combining those techniques, yeast cells (Visscher & Brakenhoff, 1991; Yevnin et al., 2013), bacteria (Visscher et al., 1993), and plant cells (Hoffmann et al., 2000) have been studied in the field of life sciences. In the physical sciences, the properties of colloids (Curran et al., 2014; Vossen et al., 2004) and fluid hydrodynamics (Curran et al., 2014; Nemet et al., 2002) have been investigated.

Recently, our group used a confocal microscope to study the effects of a NIR laser on fibroblasts plasma membrane. Confocal microscopy was used to image cell membranes and to perform fluorescence recovery after photobleaching (FRAP) experiments (Avila et al., 2018) while a continuous-wave Ti:Sa laser of 810 nm wavelength was focused on the area of interest. The NIR laser was coupled into the confocal microscope using a dichroic mirror. In this article, we report a variation of the best focus position along the optical axis provoked by the NIR laser. When the laser is turned on or off, the focus position drifts toward lower or higher values of the vertical coordinate z, respectively. Visualizations S1 and S2 on the online version of this paper show this effect: the confocal image plane on a fibroblast cell changes when the laser is turned ON.

2 | MATERIALS AND METHODS

2.1 | Experimental setup

The microscope we used is based on a Nikon Eclipse Ti inverted microscope equipped with a C1si confocal system. Briefly, the configuration was set with the following characteristics: an excitation laser of wavelength 561-nm, a Nikon oil-immersion objective Plan Apo VC 60X (1.4 numerical aperture) and a photomultiplier tube (PMT) detector to capture confocal images (see Figure 1). The sample is kept at 37°C using a temperature-controlled chamber (Tokai Hit stage top incubator). Additionally, a continuous-wave NIR laser (810 nm) is coupled into the microscope using a dichroic mirror (Semrock, FF720-SDi01-25 × 36). The NIR laser is focused by the same objective used for imaging. Its position on the sample is set using galvanometric mirrors and controlled on a CMOS camera (Thorlabs, DCC1545M) located on one of the lateral ports of the microscope. The NIR laser power stability is monitored with a power meter prior to enter the microscope. At the objective exit, the NIR power is 40 mW.

2.2 | Samples

The fluorescent dye used in the present study was FM4-64 (Invitorgen, F34653). It is generally used to stain cellular membranes because its quantum yield is two orders of magnitude higher on apolar solvents (like membrane lipids) than on polar ones like water. Images were captured on the surface of 25 mm diameter round #1-coverslips (Paul Marienfeld GmbH & Co. KG) that were previously treated with 2 μg/ml of collagen type I. The coverslip was installed inside a Chamlide magnetic chamber filled with 1.5 ml of cell culture medium plus 1 μl of FM 4–64 *solution* at 1 mg/ml in Dimethyl Sulfoxide (FM 4–64 register solution). Culture medium was used because NIH3T3 fibroblast cells were seeded on some sections of the coverslip for other experiments (Avila et al., 2018). For the present report, the fluorescent intensities were measured outside cells, on the coverslip surface, where FM4-64 showed dimmed but not null fluorescence, presumably due to the apolar portions of collagen molecules. The cell-culture solution consisted of high glucose DMEM (Dulbecco's modified Eagle's medium) plus 10% bovine-inactivate fetal serum, buffered by HEPES (N-2hydroxyethylpiperazine-N-2-ethane sulfonic acid). A droplet of immersion oil (Cargille Immersion Oil Type 37LDF) was placed between the microscope objective and the coverslip.

2.3 | Experiments

The 561-nm green scanned laser excited the dye and the fluorescence was detected by the PMT confocal detector over the spectral band ranging from 567.5 to 642.5 nm. Before each experiment, the objective was focused on the upper surface of the coverslip, that is, the bottom of the chamber containing the dye solution (see Figure 2). Images were captured at different vertical positions z of the focal plane, forming a z-stack. The confocal pinhole size was set to 60 μm. Steps between planes where either 0.5 or 0.75 μm with a time interval between each plane recording of 4.52 s (see Figure 2). The number of planes in the z-stacks varied from 5 to 12. Two conditions were studied: when the NIR laser is turned on and off, respectively. The infrared laser status (on/off) was monitored using the transmitted light detector (see Figure 1).

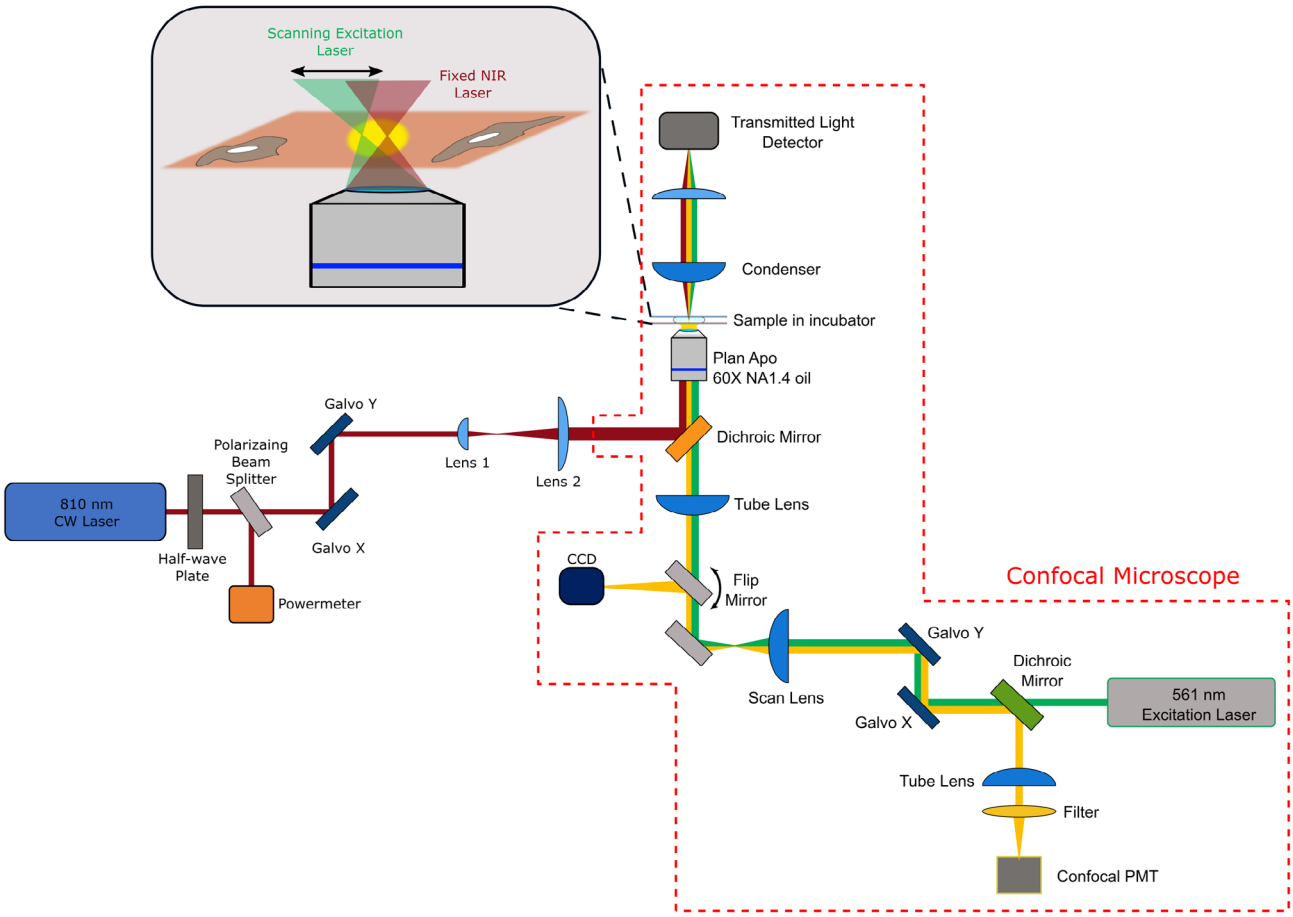

FIGURE 1 Optical setup. The instrument is based on a Nikon eclipse Ti confocal microscope (red dashed line). A 561 nm laser (represented in green rays) excites the FM4-64 dye and the emitted fluorescence (represented in yellow) is detected by confocal photomultiplier tube (PMT). A Ti:Sa laser operating in CW mode provides the 810-nm radiation (represented in red) that enters through one of the rear ports of the microscope and is reflected by a dichroic mirror. The infrared spot position is controlled with galvanometric mirrors labeled Galvo X and Galvo Y. Lenses 1 and 2 ensure beam expansion and conjugation of the galvanometric mirrors to the objective pupil. The 810-nm laser power is controlled with a half-wave plate and a polarizing beam splitter that sends one polarization direction to a power meter and the other to the microscope. The sample is mounted inside a chamber with temperature held at 37°C using a Tokai hit stage top incubator

3 | DATA ANALYSIS AND RESULTS

On each image of each *z*-stack, we measured the average fluorescence intensity inside an as large as possible region of interest (ROI) not containing any cell part nor visible cell debris (examples of such ROIs are shown in Visualizations S1 and S2 in the online version of this paper). Such measurements for one *z*-stack conform an intensity profile. The measurements are performed using a self-developed routine programmed in Jython language and run on Image J. Ten experiments were considered, each consisting of a minimum of 11 and a maximum of 34 intensity profiles. A total of 206 profiles were analyzed. For each experiment, we plotted the position (in *z* direction) versus fluorescence intensity. Examples are shown in Figure 3. The fluorescence intensity is maximum when the focus is localized on the bottom surface of the sample chamber, where the fluorescent dye lies. Let us name Z_μ this best focus position (see Figure 2). To determine Z_μ, each intensity profile was fitted with a Gaussian function and Z_μ was given the value of *z* for which the fitted function is maximum. Figure 3a,b show examples of this procedure. Values of Z_μ are then plotted against time as shown in Figure 3c,d which correspond to the data used in Figure 3a,b.

It is clearly seen that when the NIR laser is turned ON (purple points and profiles in Figures 3a,c), the best focus position drifts towards lower values of *z*. When it is turned OFF after being ON (green points and profiles in Figure 3a,c), the focus starts to return to higher values of *z*. When the NIR laser has not been turned ON in an experiment, the focus remains fairly stable. An example of that is shown in the blue profiles in Figure 3a and the corresponding data points in Figure 3c. In the first set of profiles of in Figure 3b,d the NIR laser was turned OFF but we do not know if it was ON or OFF prior to the experiment (yellow dots and profiles). In Figure 3b,d one can see that the overall focus drift can be as large as 2 μm. It is interesting to note that Z_μ values drop (when the laser ON) more rapidly than they increase (laser OFF). Data on Figure 3c,d that correspond to different status of the NIR laser are fitted with an exponential function of the form

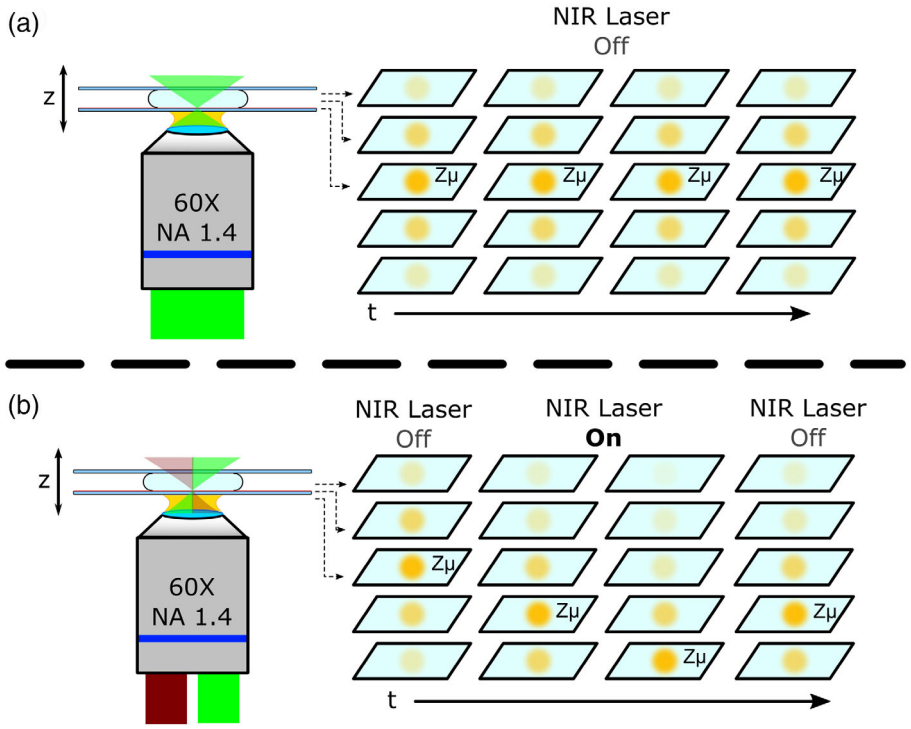

FIGURE 2 Schematic representation of the experiments used to evaluate the focus variation induced by NIR radiation. The fluorescence intensity is measured in a region of interest on several planes. Focus variation is not observed when the NIR laser is off (a) but when it is turned on (b) focus variation is observed as the position Z_μ of the maximum intensity changes

$$z_\mu(t) = c + a\left(1 - e^{-kt}\right), \tag{1}$$

which is inspired by the temporal solution of the heat equation (Guenther & Lee, 1996). Note that a is negative when the laser is ON and positive when the laser is turned OFF after having been ON.

For each measurement of Z_μ, the focus drift ΔZ_μ with respect to the focus position at the beginning of the corresponding laser status (ON or OFF) was calculated and plot against time in Figure 4. Only cases when the NIR laser was either ON (purple) or OFF after having been ON (green) are represented. A total of 128 and 78 data points are plotted for the ON and OFF states, respectively. The fitted curves obey the form of Equation (1). The values of the fitted constants are shown in Table 1. The largest registered variations of the focus position when the laser is ON and OFF are −2.25 and 0.75 μm, respectively.

4 | DISCUSSION AND CONCLUSION

The experimental evidence presented here indicates that the NIR laser light affects the focus stability of the confocal microscope. A physically plausible cause of this effect is heating provoked by the laser within the optical system, namely the combination of the microscope objective, immersion oil, and coverslip of the sample. The heat would provoke expansion and modification of the refractive index in the materials. A thermal analysis of the microscope objective was performed using Zemax OpticStudio® software. The objective optical design is described in by Yamaguchi (2003). The temperature of the lenses was varied between 20 and 47°C. The maximum variation of the consequent focus position was 0.1 μm. This result indicates that the objective is extremely well thermally compensated and that the focus variations do not come from it. Another component that could contribute to the focus variation is the coverslip. However, the material it is made of (borosilicate glass D263® M) has such low linear thermal expansion coefficient ($\alpha_l = 7.2 \times 10^{-6}\ \mathrm{K}^{-1}$) and thermal refractive index variation ($dn/dT = 2.2 \times 10^{-6}\ \mathrm{K}^{-1}$) (Rocha et al., 2016) that the effects of the NIR laser on the coverslip can be neglected in a first approximation.

Those considerations leave us with the hypothesis that the material that contributes the most to the focus variation is the immersion oil between the objective and the coverslip. Let us see if the experimental findings are consistent with a rapid theoretical calculation. The temperature variation ΔT_Q of a black body due to the absorption of heat Q is given by

$$\Delta T_Q = \frac{Q}{mC_p} \tag{2}$$

where m and C_p are the mass and the heat capacity of the body. The volume of immersion oil crossed by the laser beam is equal to $0.156\,\mathrm{mm}^3$, as shown in Data S1. Considering the oil density of $984\,\mathrm{kg\,m}^{-3}$ (Cargille-Laboratories, 2018), the mass of that oil volume is $m = 1.53 \times 10{-}7$ Kg. The heat capacity of the oil used is $C_p = 1924\,\mathrm{J\ Kg}^{-1}\ \mathrm{K}^{-1}$ (Cargille-Laboratories, 2018). The heat absorbed by the oil over a period of time Δt is

$$Q = \beta P \Delta t \tag{3}$$

where $P = 40\,\mathrm{mW}$ is the laser power at the exit of the microscope objective. Δt is chosen as the time interval for which the focus drifts

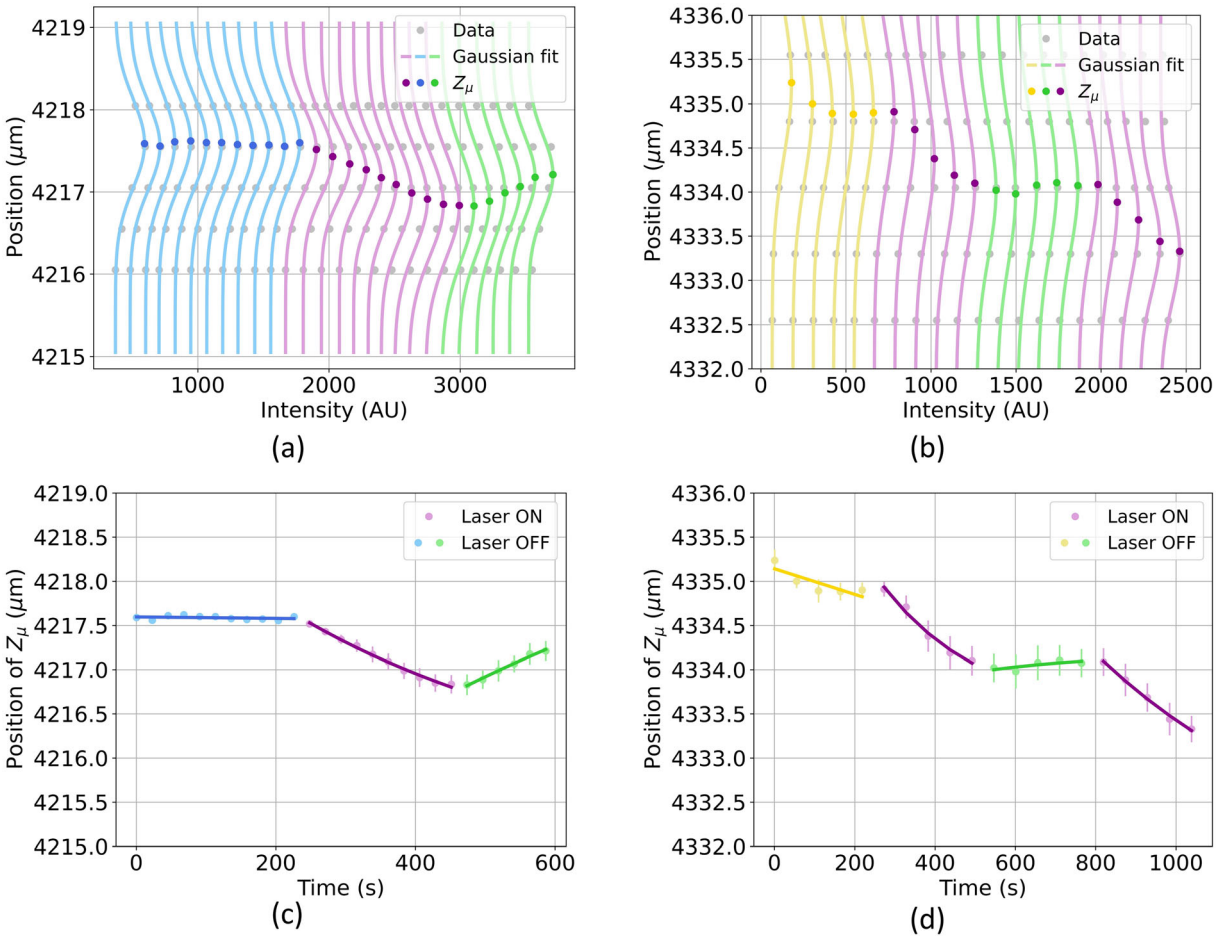

FIGURE 3 Two examples of the 10 experiments of focus variation induced by the NIR laser. Subfigures (a) and (c) correspond to one experiment, (b) and (d) to another. Intensity profiles that consist of measurements (gray dots) and fitted Gaussian curves are shown in (a) and (b). For the profiles not to appear overlapped on each other, a constant intensity value of 120 AU is added to each consecutive profile. Blue, yellow, and green colors correspond to the NIR laser being OFF and purple colors correspond to the NIR laser being ON. The most intense dots in (a) and (b) represent the locus ($z = Z_\mu$) of the maximum intensity on the gaussian fitted curves. Z_μ versus time is represented in (c) and (d). Blue indicates that the NIR laser is OFF and has been so prior to the experiment. Purple and green correspond to the NIR laser ON and then OFF, respectively. Yellow represents data where the NIR laser is OFF but its status prior to the experiment is unknown. Data in (c) and (d) are fitted with a function of the form of Equation (1)

experimentally by 1 μm when the NIR laser is ON. One can see from Figure 4, that Δt is approximately equal to 230 s. The absorption coefficient β is obtained as follows:

$$\beta = 1 - e^{-\alpha l} \tag{4}$$

where α is calculated from the reported transmittance $\tau = 0.954$ at 810 nm along a distance $x = 10$ cm as $\alpha = -\ln(\tau)/x = 0.47\,\mathrm{m}^{-1}$. The mean distance l that the laser rays travel through the immersion oil is equal to 0.24 mm. The value obtained for β is thus 1.13×10^{-4}. Using those values in Equation (3), we obtain $Q = 1.04 \times 10^{-3}$ J, which in turn leads to $\Delta T_Q = 3.5^{\circ}$C from Equation (2).

This means that considering the immersion oil as a black body, the absorption of the NIR laser over 230 s induces a temperature elevation of the oil of 3.5°C. Over that period of time, the experimental results indicate that the focus drifts by 1 μm. The increase in oil temperature can have two effects: a volumetric expansion and a modification of the refractive index. The first effect would have no impact on the thickness of the oil film because the expansion would occur toward the lateral edges of the film which have no mechanical constraint. The second effect would make the refractive index decrease, since for this oil, the $n/dT < 0$, as stated in the manufacturer data sheet (Cargille-Laboratories, 2018). The refractive index is assumed to have a linear dependence on the temperature, at least within the temperature values of interest here (from 20 to 40°C approximately). Figure 5 illustrates why a decrement in the refractive index of the oil leads to lower values of the best focus position. Let Z_μ be the distance from a fixed reference altitude to the objective lens, when the object is in perfect focus and the NIR laser is OFF (Figure 5a). With the NIR laser ON (Figure 5b), the refractive index n' of the immersion oil becomes smaller than n, the refractive index without NIR laser. Consequently, at the glass-oil interface, the rays coming from the sample

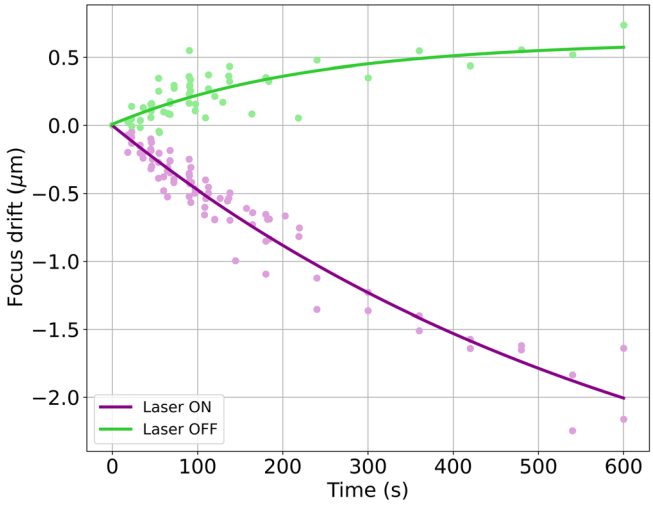

FIGURE 4 Focus drift ΔZ_μ as a function of time. ΔZ_μ values are equal to (t)$-Z_\mu$(0), where time t = 0 corresponds to the beginning of an experiment. The plot includes all the 128 and 78 measurements done with the laser ON and OFF, respectively, in 10 different experiments

TABLE 1 Fit parameters

	Parameter	
Laser status	***a* (μm)**	***k* (s^{-1})**
ON	−3.3 ± 0.4	0.0015 ± 0.0003
OFF	0.61 ± 0.09	0.004 ± 0.001

refract away from the normal interface, the rays refract away from the normal ($\beta' > \beta$), which makes the rays diverge after the objective lens and produce a blurred image. For the image to be in focus again (Figure 5c), the objective lens has to be moved away from the object, so that the outgoing rays recover parallelism. The distance Z_μ' between the reference altitude and the lens is thus shorter than Z_μ.

In Data S2, we show that the increase in temperature of the immersion oil that would produce a focus drift of 1 μm, due to the change in refractive index, is $\Delta T\_n = 2.6^\circ C$, which is of the same order of magnitude as ΔT_Q. The similarity between those numerical results indicates that the observed change in focus position is consistent with a decrease in the oil refractive index due to heating provoked by the NIR laser.

Apart from the optical effect shown here, continuous-wave NIR lasers can have effects on cellular samples. For example, the findings of Avila et al. (2018) suggest the fibroblast cellular membrane becomes more fluid when exposed to NIR laser. Blázquez-Castro (2019) give a well-documented and comprehensive review of photoxicity and thermal stress in cells and biomolecules driven by optical tweezers.

In optical trapping experiments, samples are routinely exposed for long-time periods to relatively-high power optical power on the sample ranges from a few tens to one hundred mW, like in the experiments presented here. Most of the time, those experiments are done using bright-field microscopy where a micron-change in focus may be difficult to notice. Moreover, in many experiments, the focus is actively adjusted to maintain the trapped object in focus. However,

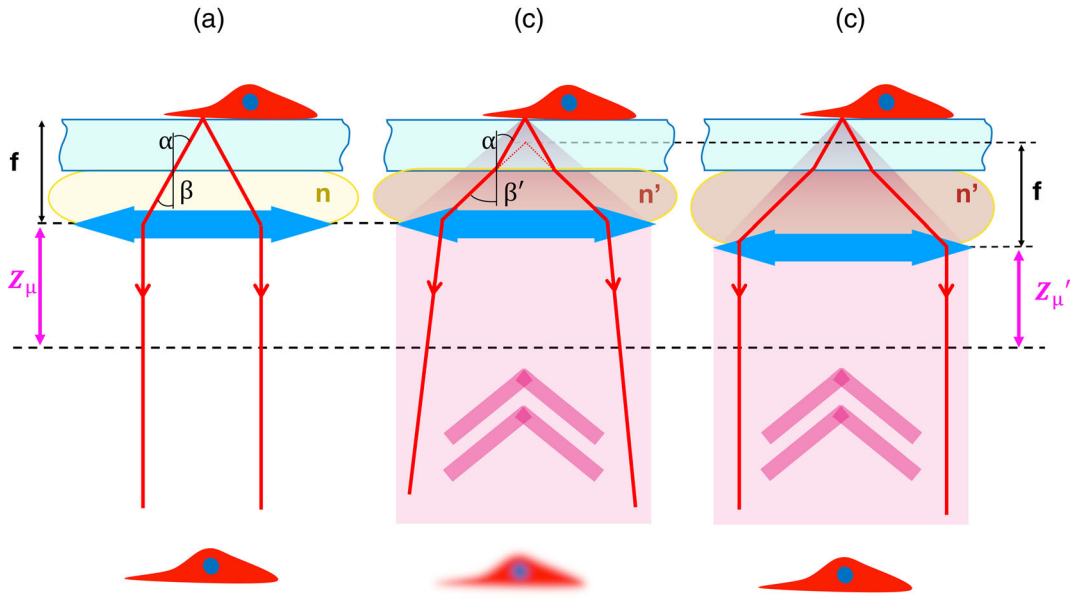

FIGURE 5 Effect of a decrement in immersion oil refractive index on the best focus position. The sample is mounted on a coverslip (light blue). The objective lens of focal length f is represented by the blue double arrow. Its position with respect to a reference altitude is Z_μ (a and b) and Z_μ' (c). Between the lens and the coverslip there is immersion oil whose refractive index is n' when crossed by the NIR laser (b and c) and n when not (a). Without NIR laser (a), the microscope forms a well-focused image of the sample. When the laser is turned ON (b), the oil refractive index n' decreases from n, the value it has when the laser is OFF (a). That makes the rays outgoing the lens to diverge. For the rays to recover parallelism and the image to be in focus again, the objective lens has to be moved away from the sample, so that $Z_\mu' < Z_\mu$

when observations are performed with confocal microscopy, focus changes are easily detected and may lead to erroneous conclusions. For example, a focus drift can provoke a change in the measured intensity that may be wrongly interpreted as an actual fluorescence variation. The effect presented here may be unnoticeable when the NIR laser is turned on during a long enough time, for the system to settle to thermal equilibrium. Moreover, automatic focus stabilization devices may be useful to compensate for the focus variations discussed in this paper.

It is pertinent to point out that if an ultra-short-pulse laser was used instead of a CW one, presumably the focus drift due to thermal effects would not be noticed, since the pulse duration is too short for the oil to warm.

Our results may be the basis of a novel method to monitor the focus stability in confocal microscopy. Fluorescent beads smaller than the point spread function of the objective lens could be inserted in the sample and used for focus monitoring. A focus variation would translate into a variation of the measured bead intensity. This bead-fluorescence method would be sensitive to refractive index fluctuations of the immersion and sample media, and to the sample-lens distance too. A potential advantage would be that no other device than the confocal microscope itself would be needed, as opposed to systems based on interferometric techniques that use an infrared diode.

AUTHOR CONTRIBUTIONS

Melissa Matrecitos-Avila: Formal analysis; investigation; methodology; software; visualization; writing – original draft. **Remy Avila:** Conceptualization; data curation; formal analysis; funding acquisition; investigation; methodology; project administration; resources; software; supervision; validation; visualization; writing – original draft; writing – review and editing. **Reinher Pimentel-Domínguez:** Formal analysis; investigation; methodology; visualization; writing – original draft. **Salvador Cuevas:** Formal analysis; investigation. **Elisa Tamariz:** Data curation; investigation. **Pablo Loza-Alvarez:** Funding acquisition; resources; writing – review and editing.

ACKNOWLEDGMENTS

The authors acknowledge financial support from CONACyT grant FORDECYT-PRONACES/1561826, UNAM-PAPIIT grants IN111815 and IN108420, CIC-UNAM, the Spanish Ministry of Economy and Competitiveness (MINECO) through the "Severo Ochoa" program for Centres of Excellence in R&D (SEV-2015-0522). Reinher Pimentel-Domínguez received a postdoctoral grant from DGAPA-UNAM. Pablo Loza-Alvarez acknowledges Fundació Privada Cellex, Fundación Mig-Puig, Generalitat de Catalunya through the CERCA program" and LASERLAB Europe (grant agreement No. 871124). Elisa Tamariz received an international stay grant from SEP, through the International Affairs Office of Universidad Veracruzana. We are deeply grateful to ICFO SLN and BIOLAB staff.

CONFLICT OF INTEREST

The authors declare no potential conflict of interests.

DATA AVAILABILITY STATEMENT

The data that support the findings of this study are available from the corresponding author upon reasonable request.

ORCID

Remy Avila https://orcid.org/0000-0002-7906-0190

REFERENCES

Avila, R., Tamariz, E., Medina-Villalobos, N., Andilla, J., Marsal, M., & Loza-Alvarez, P. (2018). Effects of near infrared focused laser on the fluorescence of labelled cell membrane. *Scientific Reports*, *8*(1), 17674.

Blázquez-Castro, A. (2019). Optical tweezers: Phototoxicity and thermal stress in cells and biomolecules. *Micromachines*, *10*, 507.

Cargille-Laboratories (2018). Immersion Oil Type 37LDF https://cargille.com/wp-content/uploads/2018/11/Immersion-Oil-Type-37LDF.pdf.

Curran, A., Tuohy, S., Aarts, D. G. A. L., Booth, M. J., Wilson, T., & Dullens, R. P. A. (2014). Decoupled and simultaneous three-dimensional imaging and optical manipulation through a single objective. *Optica*, *1*, 223–226.

Erie, J. C., McLaren, J. W., & Patel, S. V. (2009). Confocal microscopy in ophthalmology. *American Journal of Ophthalmology*, *148*, 639–646.

Guenther, R. B., & Lee, J. W. (1996). *Partial differential equations of mathematical physics and integral equations*. Dover Press.

Guida, S., Arginelli, F., Farnetani, F., Ciardo, S., Bertoni, L., Manfredini, M., Zerbinati, N., Longo, C., & Pellacani, G. (2021). Clinical applications of in vivo and ex vivo confocal microscopy. *Applied Sciences*, *11*, 1979.

Hoffmann, A., Meyer zu Hörste, G., Pilarczyk, G., Monajembashi, S., Uhl, V., & Greulich, K. O. (2000). Optical tweezers for confocal microscopy. *Applied Physics B*, *71*, 747–753.

Jerome, W. G., & Price, R. L. (Eds.). (2018). *Basic confocal microscopy*. Springer.

Jonkman, J., & Brown, C. M. (2015). Any way you slice it—A comparison of confocal microscopy techniques. *Journal of Biomolecular Techniques*, *26*, 54–65.

Jonkman, J., Brown, C. M., Wright, G. D., Anderson, K., & North, A. J. (2020). Tutorial: guidance for quantitative confocal microscopy. *Nature Protocols*, *15*, 1585–1611.

Marques, P. E., Antunes, M. M., David, B. A., Pereira, R. V., Teixeira, M. M., & Menezes, G. B. (2015). Imaging liver biology in vivo using conventional confocal microscopy. *Nature Protocols*, *10*, 258–268.

Nemet, B. A., Shabtai, Y., & Cronin-Golomb, M. (2002). Imaging microscopic viscosity with confocal scanning optical tweezers. *Optics Letters*, *27*, 264–266.

Rocha, A. C. P., Silva, J. R., Lima, S. M., Nunes, L. A. O., & Andrade, L. H. C. (2016). Measurements of refractive indices and thermo-optical coefficients using a white-light Michelson interferometer. *Applied Optics*, *55*, 6639–6643.

Stephens, D. J., & Allan, V. J. (2003). Light microscopy techniques for live cell imaging. *Science*, *300*, 82–86.

Visscher, K., & Brakenhoff, G. J. (1991). Single beam optical trapping integrated in a confocal microscope for biological applications. *Cytometry. Part A: the journal of the International Society for Analytical Cytology*, *12*, 486–491.

Visscher, K., Brakenhoff, G. J., & Krol, J. J. (1993). Micromanipulation by "multiple" optical traps created by a single fast scanning trap integrated with the bilateral confocal scanning laser microscope. *Cytometry. Part A: the journal of the International Society for Analytical Cytology*, *14*, 105–114.

Vossen, D. L., van der Horst, A., Dogterom, M., & van Blaaderen, A. (2004). Optical tweezers and confocal microscopy for simultaneous three-dimensional manipulation and imaging in concentrated colloidal dispersions. *Review of Scientific Instruments*, *75*, 2960–2970.

Yamaguchi, K. (2003). U.S. Patent No. 6519092B2. Washington, DC: U.S. Patent and Trademark Office.

Yevnin, M., Kasimov, D., Gluckman, Y., Ebenstein, Y., & Roichman, Y. (2013). Independent and simultaneous three-dimensional optical trapping and imaging. *Biomedical Optics Express*, *4*, 2087–2094.

SUPPORTING INFORMATION

Additional supporting information can be found online in the Supporting Information section at the end of this article.

How to cite this article: Matrecitos-Avila, M., Avila, R., Pimentel-Domínguez, R., Cuevas, S., Tamariz, E., & Loza-Alvarez, P. (2022). Focus variation due to near infrared laser in a confocal microscope. *Microscopy Research and Technique*, *85*(10), 3431–3438. https://doi.org/10.1002/jemt.24198